Role of Surfactants in Carbon Nanotubes Density Gradient Separation

Elton J. F. Carvalho and Maria Cristina dos Santos*

Departamento de Física dos Materiais e Mecânica, Instituto de Física, Universidade de São Paulo, 05315-970 São Paulo SP, Brazil

Carbon nanotubes are known, among several properties, to be hydrophobic molecules and thus do not dissolve in water. Usually, these long, narrow carbon cylinders are closed at the ends and interact with each other through van der Waals interactions. The samples obtained by the commonly used synthetic methods are formed by nanotube bundles containing a variety of diameters and chiralities. The effective use of carbon nanotubes in many technological applications relies either on the availability of large scale sorting methods or selective growth methods, in order that uniform samples are obtained. Progress in these areas has recently been reviewed by Hersam.[1]

An important sorting method was developed by Arnold and collaborators,[2] by which nanotubes are dispersed in detergent solutions. Being hydrophobic, SWNTs do not dissolve in water without the help of surfactants, which are amphiphilic molecules that are able to bind to hydrophobic species and at the same time are attracted to water. Ultrasound waves are still needed to break the bundles and allow the surfactants to wrap on the tubes and effectively suspend them in water. The sorting by diameter or by electronic structure was carried out by ultracentrifugation of these dispersions inside a density gradient. The sorting process was successful when SC was used to suspend nanotubes, and cosurfactant mixtures, when used, were added just before ultracentrifugation. It seems that the specific way surfactants bind to the nanotube walls is relevant to the ultracentrifugation outcome. Experimentally, it was found that the solubility of nanotubes in SDS solutions decreases with increasing centrifugation force.[3] Recent molecular dynamics

studies of the nanotube/SDS system in water showed that these amphiphiles form aggregates over the molecules already adsorbed on the walls such that surface coverage is not uniform.[4]

It has been pointed out by Rinzler,[5] however, that nanotube distribution along the density gradient occurs in the opposite direction to what would be expected on the basis of the relationship between nanotube density and diameter. The density of surfactant-encapsulated nanotubes should decrease with increasing nanotube diameter, when the nanotubes are empty. As a consequence, larger diameter tubes were expected to be found up in the low density part of the centrifuge tube, but they are actually found in the high density part. A hydrodynamical model was recently developed to account for this apparent contradiction.[6]

ABSTRACT   Several strategies aimed at sorting single-walled carbon nanotubes (SWNT) by diameter and/or electronic structure have been developed in recent years. A nondestructive sorting method was recently proposed in which nanotube bundles are dispersed in water—surfactant solutions and submitted to ultracentrifugation in a density gradient. By this method, SWNTs of different diameters are distributed according to their densities along the centrifuge tube. A mixture of two anionic amphiphiles, namely sodium dodecylsulfate (SDS) and sodium cholate (SC), presented the best performance in discriminating nanotubes by diameter. We present molecular dynamics studies of the water—surfactant—SWNT system. The simulations revealed one aspect of the discriminating power of surfactants: they can actually be attracted toward the interior of the nanotube cage. The binding energies of SDS and SC on the outer nanotube surface are very similar and depend weakly on diameter. The binding inside the tubes, on the contrary, is strongly diameter dependent: SDS fits best inside tubes with diameters ranging from 8 to 9 Å, while SC is best accommodated in larger tubes, with diameters in the range 10.5—12 Å. The dynamics at room temperature showed that, as the amphiphile moves to the hollow cage, water molecules are dragged together, thereby promoting the nanotube filling. The resulting densities of filled SWNT are in agreement with measured densities.

KEYWORDS: molecular dynamics · carbon nanotube density · surfactants

Experiments carried out by Wenseleers and collaborators[7] have offered an alternative explanation to the inverted density × diameter relationship of the ultracentrifugation sorting. They have shown that the ultrasound waves provoke the breaking of the tube ends. As much as 40% of nanotubes were reported to open after 15 min of sonication. Furthermore, spectroscopic characterization of samples treated by sonication is consistent with the open tubes being filled with water. Another set of sorting experiments and a molecular dynamics (MD) study was carried out by Hennrich et al.[8] Water was allowed to enter SWNTs of several diameters in MD simulations. The authors obtained a layered structure of water molecules inside the tubes and a filled tube density that still decreased with tube diameter. Better results were obtained supposing that the surfactant shell outside the tubes provokes a charge transfer (assumed to be −0.1 e/carbon atom), resulting in a negatively charged tube. This allows more water molecules to enter the tubes, which contributes to increase the density and gives a qualitative interpretation to the inverted density × diameter relationship.

We further explored this problem by studying the interaction of surfactant molecules with SWNTs. Molecular dynamics with a suitable force field, as described below, was used to investigate the interaction of the nanotube−surfactant systems, both isolated and surrounded by water. Three amphiphiles were considered: those used by Arnold et al., SDS and SC, and an aromatic and nonionic amphiphile, 2,3-bis[2-methoxyethyl]-naphthalene (MEN). The latter surfactant was chosen because of its aromatic apolar segment, which should increase the adhesion to the nanotube surface and also because it is nonionic.[9] The simulations of the isolated pair considered one nanotube and one surfactant molecule while the simulations in the presence of water were carried out adopting periodic boundary conditions. The simulation box was filled with enough water molecules to obtain a water density of 1 g/cm^3 surrounding the nanotube−surfactant solute. Charge neutrality was always imposed by adding sodium cations together with anionic amphiphiles. Although the anionic amphiphiles considered here hydrolyze giving the surfactant solutions a slight basic character (natural pH ≈ 8 at the usual concentrations), we did not try to simulate different pH conditions since the photoluminescence of dispersed SWNTs does not change in pH values ranging from 7 to 12.[10]

RESULTS AND DISCUSSION

The first set of calculations, whose results are displayed in Figure 1, consisted of structure optimizations involving various SWNT geometries and the surfactant molecules. The amphiphiles were allowed to interact with nanotubes in two distinct situations: at the outer tube surface (open symbols in Figure 1), and inside the
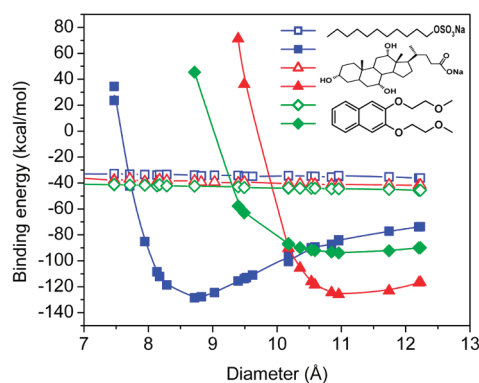

Figure 1. Binding energies (kcal/mol) as a function of nanotube diameter (Å). Open symbols: surfactant adhered to the outer nanotube surface. Full symbols: surfactant inside the nanotube cavity. The surfactant molecular structures are sketched beside the labels: blue symbols, SDS; red symbols, SC; green symbols, MEN.

tube (full symbols in Figure 1). The binding energy of the SWNT-surfactant system was calculated as

$$BE = E_{SWNT+surf} - (E_{SWNT} + E_{surf}) \qquad (1)$$

where $E_{SWNT+surf}$ is the minimum energy of the SWNT+surfactant system and E_{SWNT} and E_{surf} are the minimum energies of the isolated molecules. By this definition, more negative BE values imply more stable configurations.

The surfactant molecular structures are sketched beside the labels in Figure 1. We notice first that these molecules present similar binding energies at the outer nanotube surface, although a noticeable preference for more planar surfactant structure can be deduced. In other words, MEN binding to SWNT is stronger than SC and SDS binding. The evolution is toward stronger binding as the tube diameter increases, in all three cases, due to the decreasing curvature. An important difference was obtained when the surfactant is inside the tube, as demonstrated by the curves with full symbols. Owing to geometrical constraints, these surfactants are not allowed inside tubes whose diameters are smaller than a critical diameter, which depends on the radius of gyration of each molecule. Assuming that this critical diameter corresponds to zero BE (see eq 1), one obtains 7.5 Å for SDS, 9.0 Å for MEN, and 9.7 Å for SC. MD simulations were also carried out in vacuo in order to verify whether the surfactant molecule could be attracted to the tube interior or not, in case any barrier would prevent it to happen. These simulations were run in a canonical ensemble (constant number of particles, volume, and temperature, NVT) at 300 K. The open-end (14,0) nanotube, which has a diameter of 10.7 Å, was used. All surfactants, when approached the open end, were attracted to the internal region. It is interesting to note that the surfactant travels inside the tube until the opposite open end is reached, when it is attracted back to the interior of the tube. The surfactant kinetic energy is gradually transferred to the SWNT's vibra-
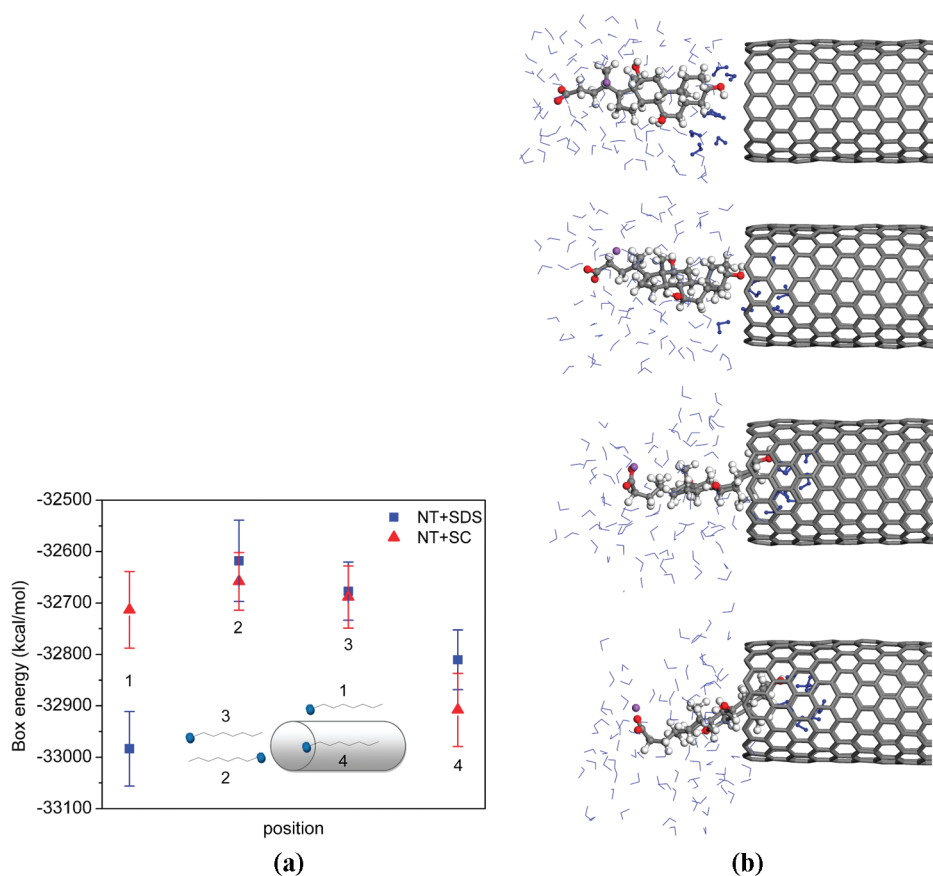
Figure 2. Solvation effects and water pumping into the nanotube. (a) Average potential energy (kcal/mol) of the simulation box, at 300 K, of the solvated (14,0) nanotube−surfactant system in four configurations: (1) surfactant at the outer nanotube surface; (2) surfactant close to the nanotube open end, polar head first; (3) surfactant close to the nanotube end, apolar tail first; (4) surfactant inside the nanotube cavity. The bars represent the standard deviations due the energy fluctuation. Blue symbols, SDS; red symbols, SC. **(b)** Molecular dynamics snapshots involving a (15,0) SWNT and SC with a solvation layer containing 92 water molecules, displayed as the blue structures. The highlighted water molecules are pushed by the surfactant in its trajectory toward the nanotube interior. Time interval between consecutive snapshots is 10 ps.

tional modes, *via* the van der Waals interactions, such that the oscillatory motion is dampened. This leads to the surfactant eventually coming to rest inside the SWNT.

We now turn to the investigation of water effects in the surfactant binding to SWNT. This was done in the second set of calculations, where water molecules were explicitly included in the simulation box. Typical results are displayed in Figure 2a. Here we show time averages of the total box potential energy, as well as the standard deviation, in several configurations of the SWNT−surfactant system, as indicated in the sketch included in Figure 2a. Results are for the (14,0) nanotube (diameter of 10.7 Å) interacting with SDS and SC. These were particularly long simulations due to the large number of atoms. During the simulations at 300 K, water molecules did not enter the tube. SDS in configuration 1, that is, when it is adsorbed at the outer nanotube surface, has the lowest potential energy, while SC reaches the lowest potential energy at configuration 4, that is, inside the nanotube cavity. Although the isolated pair SDS-SWNT with this particular tube has lower energy when SDS lies inside it, as seen in Figure 1, the

interaction with water changes the relative stability and favors SDS binding at the outer SWNT surface. The solvated SC-SWNT, on the other hand, has SC inside the tube as the lowest potential energy configuration. Similar calculations were performed for SDS interacting with the (7,5) nanotube (diameter 8.2 Å) in water. At this tube diameter, according to the results shown in Figure 1, the binding of SDS to the nanotube cavity in vacuum is the largest. The potential energy averages resulted similar to those obtained for SC-SWNT, namely, SDS in configuration 4 having the smallest potential energy. Concluding, the average potential energies of several nanotube−surfactant configurations in water are consistent with the amphiphile preferring the inner cavity when the nanotube diameter is close to that corresponding to largest binding energy, otherwise the interaction with water favors the binding at the outer surface. This clearly shows a diameter selectivity of surfactants.

We first investigated the dragging of the surfactant toward the nanotube cavity without water. In water solutions, when the amphiphile is attracted to the interior of a nanotube, driven by the van der Waals forces,
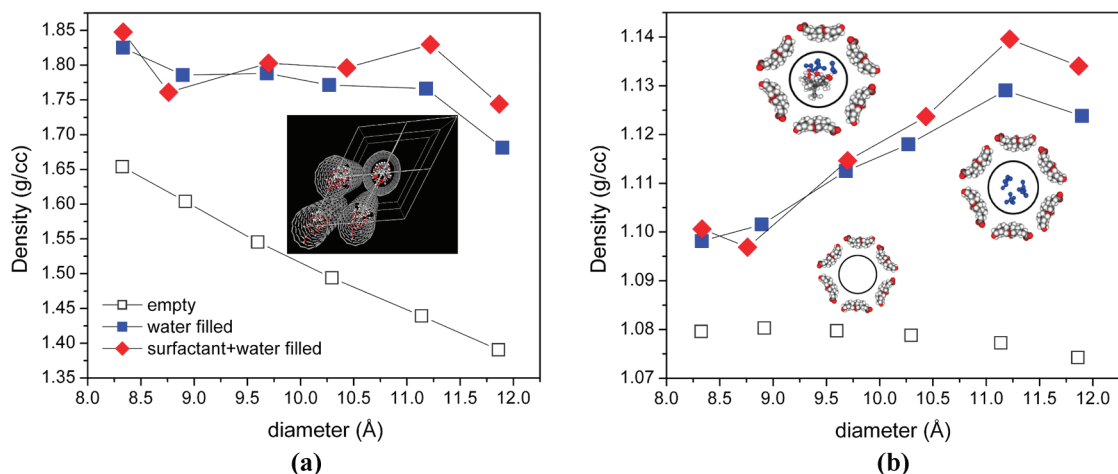
Figure 3. (a) Densities obtained from unit cell optimizations of SWNTs: empty nanotubes (open squares), water filled (full squares), and surfactant+water filled (full diamonds) nanotubes. The inset illustrates the hexagonal packing of SWNT crystals. **(b)** Densities of suspended nanotubes including a surfactant shell, calculated from eq 2. Symbols as in panel a.

the surrounding water molecules should also be indirectly attracted through the interaction with the amphiphile. We were not able to find trajectories supporting this hypothesis in the large box simulations reported above, because it would take an enormous amount of simulation time. Then we simplified the simulation box by including only the nanotube and the surfactant surrounded by 92 water molecules. The amphiphile and the solvation layer were then allowed to approach the open end of a (15,0) nanotube. Some snapshots of the trajectory are displayed in Figure 2b. Water molecules are represented by the blue structures. The highlighted molecules are pushed into the nanotube cavity as the amphiphile moves toward the interior of the SWNT. The ultrasound waves and the extreme forces during ultracentrifugation should further help the filling. We also simulated the same water cluster without the surfactant and water did not enter the nanotube. Water inside nanotubes has been the subject of several studies.[8,11,12] In particular, MD simulations showed that small variations in the van der Waals parameters describing carbon−water interaction can change the results from filled nanotubes to empty nanotubes immersed in water.[11] The advantage of having amphiphiles inside the SWNTs together with water is that the system may adopt a denser packing than the layered water structure formed inside the hydrophobic cavity.[8,13] Therefore the nanotube density is increased.

These results suggest that the surfactants discriminate nanotubes by diameter by selectively filling the nanotube cavity according to the relationship between the surfactant radius of gyration and the nanotube diameter. This implies that SDS most probably fills smaller diameter nanotubes while SC should fill larger diameter nanotubes. As a matter of fact, Arnold et al.[2] reported an enhanced isolation of larger diameter SWNTs when SC was used alone, and an enhanced isolation of smaller diameter SWNTs in a mixture of SDS and SC with the weight ratio 1:4. It remains to be evaluated how

the surfactant plus water filling affects nanotube density. For this purpose we performed constant pressure molecular dynamics calculations (NPT) at room temperature to obtain the average number of water molecules (or water plus surfactant) inside SWNTs in equilibrium with water in a large simulation box. We note that surfactant solutions inside nanotubes have already been studied through molecular dynamics simulations,[13−15] in large diameter nanotubes. One of these studies[13] has shown that the SDS hydrophobic tail adheres to the inner surface while the polar head points to center, allowing a high packing of water through electrostatic interactions with the polar heads and the counterions. In our systems there is not much room left inside the nanotubes for surfactants to adhere to the inner surface and decrease the hydrophobicity of the cavity.

We assumed that nanotubes having less than 10 Å of diameter can only be filled with SDS and the larger ones were filled with SC only, according to the results of Figure 2a. After we obtained the average number of water plus surfactant inside a finite open-ended nanotube, we built infinite nanotubes whose unit cell contained the same average number of molecules per unit length in the tube cavity. Then we arranged the nanotubes in a triangular lattice to perform solid state structure minimizations resulting in a solid state density (the mass of the unit cell divided by the unit cell volume), to be compared with the density of empty nanotube solids, and nanotube solids filled with water only. The results are displayed in Figure 3a. Notice that while empty nanotube densities decrease with increasing diameter, the filling with water has the effect of diminishing the decrease rate and the water−surfactant mixture *increases* the density as diameter increases. The optimal number of molecules that can fill the nanotubes grows stepwise, causing the ups and downs in the density profile. The density of suspended nanotubes was considered to depend upon a SC shell of

thickness t and density ρ_{shell} that covers the outer nanotube surface according to the formula

$$\rho = \frac{\rho_{solid} \times D^2 + \rho_{shell} \times [(D + 2t)^2 - D^2]}{(D + 2t)^2} \quad (2)$$

where ρ_{solid} is the nanotube density obtained in the solid state minimization (Figure 3a) and D is the corresponding diameter. The van der Waals distance between the nanotube wall and its surroundings is already included in ρ_{solid}. We measured the shell thickness from our simulations and obtained $2t \approx 17$ Å. The SC shell has a surfactant packing around the nanotubes consistent with that of the literature.[16] The resulting shell density, that takes into account the surfactants and its hydration layer, is close to that of water, $\rho_{shell} \approx 1.01$ g/cm^3. The results are displayed in Figure 3b. Overall, the calculated densities of empty, water-filled and water+surfactant-filled nanotubes show that the filling is needed to obtain a density that increases with diameter and the values are within the experimentally measured densities.[2] We recall that these densities were obtained considering full occupation of the nanotube cavity, so that they represent the largest possible densities.

We believe that the present model gives a rather good interpretation of the inverted density $\times$ diameter relationship and shows how amphiphiles discriminate among nanotubes of diverse diameters. There are questions about the sorting process of SWNTs that classical molecular dynamics cannot answer. The sorting by electronic structure is certainly related to the mechanisms discussed above but a more detailed investigation will require quantum chemical studies due to the complex electronic structures of SWNTs.[17] The combination of classical MD with *ab initio* techniques to study amphiphile−SWNT interactions should prove helpful to the improvement of sorting methods.

METHODS

All MD calculations and structure optimizations were carried out using the CVFF-950[18] force field as implemented in Cerius2[19] package. Bonding parameters for water molecules were taken from CVFF force field and atomic charges from the SPC[20] water model. Calculations included valence terms (bond stretch, bond angle, torsion angle), as well as van der Waals and Coulomb terms. Since CVFF is known[21] to reproduce hydrogen bond behavior well enough when atomic charges are correctly assigned, no explicit hydrogen bond energy terms need to be taken into account. Charge distributions in surfactant molecules were calculated *via* Rappé−Goddard[22] charge equilibration scheme of the isolated molecule at the equilibrium geometry and kept frozen during energy minimization procedures and solvated MD. For SDS and SC, ionized (organic anion separated from sodium cation) surfactant molecules were used in MD simulations.

Constant volume (NVT) and constant pressure (NPT) MD simulations were performed at 300 K, with a time step of 1 fs. The temperature control was made by the Nosé−Hoover algorithm.[23] The water filling of the simulation box measuring $35 \times 35 \times 90$ Å^3 started by the hexagonal ice crystalline structure. The system was driven to thermal equilibrium, that is, until the radial distribution of water oxygen atoms reproduced that of the literature,[24] after around 20 ps. A cylindrical void of an appropriate diameter was created in the center of the box to accommodate the nanotube. After this process, the periodic box contained of the order of 3300 water molecules and 700 carbon atoms from the SWNT. A second void was created to include the surfactant, when needed.

The large simulation box described above was used to calculate potential energy averages and standard deviations. We proceeded with an energy minimization of the simulation box, considering the water molecules as rigid bodies, until the average force dropped below 0.5 kcal/(mol Å). The energy-minimized box was then thermalized for 10 ps at 300 K. The initial atom velocities were randomly assigned from a 600 K Maxwell−Boltzmann distribution. The atomic positions and velocities from the last frame of the thermalization run were used as initial conditions for the production, average-taking run, which lasted 5 ps, and data were recorded every 10 time steps (10 fs), resulting in 500 data points for potential energy average and standard deviation evaluation.

REFERENCES AND NOTES

1. Hersam, M. C. Progress Towards Monodisperse Single-Walled Carbon Nanotubes. *Nat. Nanotechnol.* **2008**, *3*, 387–394.
2. Arnold, M. S.; Green, A. A.; Hulvat, J. F.; Stupp, S. I.; Hersam, M. C. Sorting Carbon Nanotubes by Electronic Structure Using Density Differentiation. *Nat. Nanotechnol.* **2006**, *1*, 60–65.
3. Ke, P. C. Fiddling the String of Carbon Nanotubes with Amphiphiles. *Phys. Chem. Chem. Phys.* **2007**, *9*, 439–447.
4. Tummala, N. R.; Striolo, A. SDS Surfactants on Carbon Nanotubes: Aggregate Morphology. *ACS Nano* **2009**, *3*, 595–602.
5. Rinzler, A. G. Materials Processing: Sorting out Carbon Nanotube Electronics. *Nat. Nanotechnol.* **2006**, *1*, 17–18.
6. Nair, N.; Kim, W.-J.; Braatz, R.; Strano, M. Dynamics of Surfactant-Suspended Single-Walled Carbon Nanotubes in a Centrifugal Field. *Langmuir* **2008**, *24*, 1790–1795.
7. Wenseleers, W.; Cambré, S.; Čulin, J.; Bouwen, A.; Goovaerts, E. Effect of Water Filling on the Electronic and Vibrational Resonances of Carbon Nanotubes: Characterizing Tube Opening by Raman Spectroscopy. *Adv. Mater.* **2007**, *19*, 2274–2278.
8. Hennrich, F.; Arnold, K.; Lebedkin, S.; Quintillá, A.; Wenzel, W.; Kappes, M. M. Diameter Sorting of Carbon Nanotubes by Gradient Centrifugation: Role of Endohedral Water. *Phys. Status Solidi* **2007**, *244*, 3896–3900.
9. Mallik, A.; Lee, S.; Tran, L.; Lobkovsky, E. Crystal Topology Prediction in Alternating Amphiphiles: Aromatic Polyethers and the Role of Volume Fraction. *Cryst. Growth Des.* **2003**, *3*, 467–473.
10. Okazaki, T.; Saito, T.; Matsuura, K.; Ohshima, S.; Yumura, M.; Iijima, S. Photoluminescence Mapping of "As-Grown" Single-Walled Carbon Nanotubes: A Comparison with Micelle-Encapsulated Nanotube Solutions. *Nano Lett.* **2008**, *5*, 2618–2623.
11. Hummer, G.; Rasaiah, J.; Noworyta, J. Water Conduction through the Hydrophobic Channel of a Carbon Nanotube. *Nature* **2001**, *414*, 188–190.
12. Koga, K.; Gao, G. T.; Tanaka, H.; Zeng, X. C. Formation of Ordered Ice Nanotubes Inside Carbon Nanotubes. *Nature* **2001**, *412*, 802–805.

13. Tummala, N. R.; Striolo, A. Curvature Effects on the Adsorption of Aqueous Sodium-Dodecyl-Sulfate Surfactants on Carbonaceous Substrates: Structural Features and Counterion Dynamics. *Phys. Rev. E* **2009**, *80*, 0214081−10.

14. Arai, N.; Yasuoka, K.; Zeng, X. C. Self-Assembly of Surfactants and Polymorphic Transition in Nanotubes. *J. Am. Chem. Soc.* **2008**, *130*, 7916–7920.

15. Zhang, X.; Cao, D.; Wang, W. Formation of New Morphologies of Surfactant−Inorganic−Water Systems under Spherical Confinements. *J. Phys. Chem. C* **2008**, *112*, 2943–2948.

16. Arnold, M. S.; Suntivich, J.; Stupp, S. I.; Hersam, M. C. Hydrodynamic Characterization of Surfactant Encapsulated Carbon Nanotubes Using an Analytical Ultracentrifuge. *ACS Nano* **2008**, *2*, 2291–2300.

17. Friddle, R. W.; Lemieux, M. C.; Cicero, G.; Artyukhin, A. B.; Tsukruk, V. V.; Grossman, J. C.; Galli, G.; Noy, A. Single Functional Group Interactions with Individual Carbon Nanotubes. *Nat. Nanotechnol.* **2007**, *2*, 692–697.

18. Dauber-Osguthorpe, P.; Roberts, V. A.; Osguthorpe, D. J.; Wolff, J.; Genest, M.; Hagler, A. T. Structure and Energetics of Ligand Binding to Proteins: *Escherichia coli* Dihydrofolate Reductase-Trimethoprim, a Drug-Receptor System. *Proteins: Structure, Funct. Genet.* **1988**, *4*, 31–47.

19. *Cerius²*, version 4.10; Accelrys, Inc: San Diego, CA, 2005.

20. Guillot, B. A Reappraisal of What We Have Learnt During Three Decades of Computer Simulations on Water. *J. Mol. Liq.* **2002**, *101*, 219–260.

21. Hobza, P.; Kabeláč, M.; Šponer, J.; Mejzlík, P.; Vondrášek, J. Performance of Empirical Potentials (AMBER, CFF95, CVFF, CHARMM, OPLS, POLTEV), Semiempirical Quantum Chemical Methods (AM1, MNDO/ M, PM3), and *ab Initio* Hartree−Fock Method for Interaction of DNA Bases: Comparison with Nonempirical Beyond Hartree−Fock Results. *J. Comput. Chem.* **1996**, *18*, 1136–1150.

22. Rappé, A. K.; Goddard, W. A., III. Charge Equilibration for Molecular Dynamics Simulations. *J. Phys. Chem.* **1991**, *95*, 3358–3363.

23. Hoover, W. G. Canonical Dynamics: Equilibrium Phase-Space Distributions. *Phys. Rev. A* **1985**, *31*, 1695–1697.

24. Head-Gordon, T.; Hura, G. Water Structure from Scattering Experiments and Simulation. *Chem. Rev.* **2002**, *102*, 2561–2670.